Synthesis and Formation of Silica Aerogel Particles By a Novel Sol−Gel Route in Supercritical Carbon Dioxide

Ruohong Sui,[†] Amin S. Rizkalla,*[,†,‡] and Paul A. Charpentier*[,†]

Department of Chemical and Biochemical Engineering, Faculty of Engineering, University of Western Ontario, London, Ontario, Canada N6A 5B9, and Division of Biomaterials Science, University of Western Ontario, London, Ontario, Canada N6A 5B9

Received: October 3, 2003; In Final Form: May 30, 2004

A new method to obtain silica aerogel particles using acetic acid as the condensation agent for silicon alkoxides in supercritical carbon dioxide ($scCO_2$) is proposed. The objective of this study was to determine the mechanism of silica aerogel formation in $scCO_2$ using in situ analysis techniques. The synthesis and formation of silica aerogel particles was carried out by a modified sol−gel route, based on the hydroxylation and condensation of silicon alkoxides in $scCO_2$; both submicron and micron-size aerogel spheres were obtained. By means of in situ Fourier Transform infrared spectroscopy (FTIR), the activity of acetic, formic, benzoic, and chloroacetic acids were studied for the condensation of tetraethyl orthosilicate (TEOS). Formic and acetic acid gave slower rates than benzoic and chloroacetic acids. Increasing the concentration of acid and addition of extra water led to an acceleration of the reaction. The reactions were also studied as a function of temperature and pressure. Higher rates of reaction were obtained at higher temperatures and lower pressures. Results from particle formation studies indicated that by slowing the rate of reaction, precipitation and agglomeration of particles could be minimized. A submicron particle size range was obtained by depressurization of the sol−gel solution inside the reaction vessel, while the rapid expansion of supercritical solutions (RESS) process was found to yield particles in the size range of approximately 100 nm.

Introduction

The use of supercritical fluids (SCFs) for the processing of materials has attracted considerable interest in recent years.[1−3] Of the supercritical fluids, the most exciting potential is provided by the environmentally friendly solvent, supercritical carbon dioxide ($scCO_2$). It is generating a great deal of industrial interest for several applications, including polymer synthesis, hydrogenation, drycleaning of clothes, silicon chip cleaning, microelectronics, polymer foam extrusion, neutraceuticals, and particle formation.[4−10] This is because $scCO_2$ is inexpensive, of low toxicity, nonflammable, and environmentally and chemically benign. The solubility of various compounds in $scCO_2$ can also be altered dramatically by relatively small changes in total pressure and/or temperature, hence $scCO_2$ is a "tunable solvent".[11] In addition, supercritical fluids can be easily separated from both organic cosolvents and solid products providing a potential clean, recyclable, and environmentally friendly technology.

High diffusivity and low viscosity in supercritical fluids is considered highly effective for producing superior products of fine and uniform particles.[12] In particle formation, SCFs offer many opportunities to form particles with improved properties. From a processing aspect, producing particles by SCFs can be classified into several major processes such as GAS, RESS, PGSS, SEDS, etc.[7,13] For example, the GAS process uses the SCF as an anti-solvent to precipitate particles from a solution of the material in an organic solvent;[14] while in the RESS process,[15−19] product molecules are solvated in the SCF that nucleate and form clusters when the fluid rapidly goes through a nozzle and is depressurized.

Designing new and improved silica aerogel particles has many potential applications, such as catalyst matrixes, chromatography resins, and precursors for ceramic powders for biomaterials.[20−23] An aerogel is a gel that has a lower density than the fully condensed form of the material forming it. Aerogels are typically produced by replacing the liquid of a gel by air or another gas without allowing complete collapse of the structure.[24] Early work led to aerogels through the use of supercritical fluids to extract liquid, and it led to the hypothesis that the gel structure itself can be preserved in the supercritical drying process.[25] Silica aerogels are conventionally prepared by hydrolyzing and condensing silicon alkoxides in water and/or organic solvents under ambient pressure with an inorganic acid or base as catalyst, gelating for a long time, then drying in $scCO_2$.[26,27] A route of silica aerogel particle synthesis was previously developed using formic acid to react with tetramethyl orthosilicate (TMOS) or tetraethyl orthosilicate (TEOS) in a supercritical fluid. The first monolithic silica aerogel was synthesized by employing this methodology in 1997,[28] and M. Moner-Girona et al.[29] in 2003 obtained micron-size spheres and fibers in supercritical acetone, but found it difficult to have separated particles in $scCO_2$ because of agglomeration. Advantages of this route include a shorter time for gel aging, obtaining dry product directly after CO_2 venting, and the ability of the size and morphology of the silica aerogel to tailored by modifying the temperature, pressure, relative amounts of reactants, and supercritical fluid venting rate. However, the mechanism and kinetics of the reactions are not well understood.

* To whom correspondence should be addressed. E-mail: pcharpentier@eng.uwo.ca, arizkalla@eng.uwo.ca. Phone: (519) 661-3466, (519) 661-2111 x 82212. Fax: (519) 661-3498.

[†] Department of Chemical and Biochemical Engineering, University of Western Ontario.

[‡] Division of Biomaterials Science, University of Western Ontario.

10.1021/jp036973d CCC: $27.50
Published on Web 07/16/2004

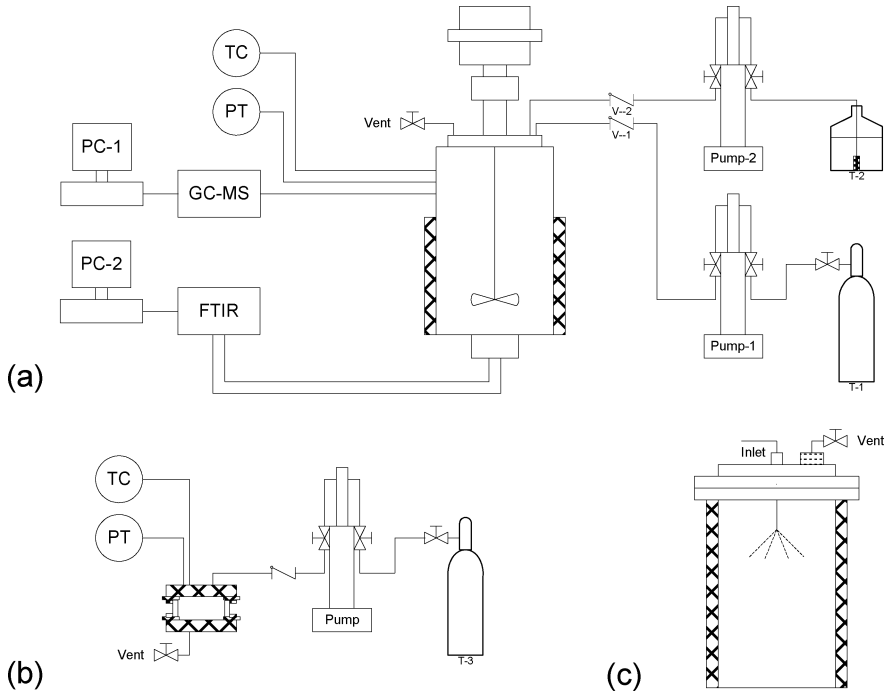

Figure 1. Schematic of experiment setup: (a) autoclave with FTIR and GC-MS, (b) view cell system, (c) particle collection device for the RESS process. (T-1, T-3) CO_2 cylinders, (T-2) liquid reactant tank, (Pump) syringe pump, (PT) pressure transducer, (TC) temperature controller.

Recent literature has shown that attenuated total reflection Fourier transform infrared (ATR-FTIR) spectroscopy is technically feasible for in situ measurement of concentration, solubility, and supersaturation in crystallization processes for the chemical and pharmaceutical industries.[30,31] ATR spectroscopy uses the phenomenon of total internal reflection. In this technique, the radiation beam is directed onto an angled crystal and reflected within the crystal until it emerges from the other "end", where it is collected. The depth of penetration, as the beam of radiation penetrates a fraction of a wavelength beyond the reflecting surface, distinctively produces (a) little to nondisturbing interference from the solid particles already present in the solution, or generated by crystallization, and (b) a less intense solvent contribution to the overall infrared spectrum so the solvent spectra can be easily subtracted from the sample spectrum. These characteristics of small depth of penetration with no sensitivity to solid particles constitute the technical motivation for the employment of ATR-FTIR technology as an online monitoring tool for supercritical crystallization.

Combining sol−gel science with SCF technology provides an opportunity to synthesize new and improved aerogel particles from silicon alkoxides in $scCO_2$. The goal of the present work was (1) to investigate the technical potential and efficacy of ATR-FTIR spectroscopy for the in situ monitoring of solute concentration during the modified aerogel procedure in $scCO_2$, and (2) to study the particle formation by means of two techniques of (a) destabilizing the sol−gel solution by pressure reduction and (b) the RESS process.

Materials and Methods

Materials. Reagent-grade tetraethyl orthosilicate (TEOS), tetramethyl orthosilicate (TMOS), acetone (HPLC grade), acetic, benzoic acid, and chloroacetic acid were obtained from the Aldrich Chemical Co. (Ontario, Canada), and used without further purification. Formic acid (Aldrich, reagent grade) was further dehydrated by refluxing with phthalic anhydride (Sigma-Aldrich, 99% reagent grade) for 6 h and then distilling. Instrument-grade carbon dioxide (99.99%) was obtained from BOC Canada and further purified by passage through columns containing molecular sieves (Aldrich) and copper (II) oxide supported on alumina (Aldrich) to remove excess water and oxygen, respectively. Purified water was produced by means of a 18.2 Mohm-cm Barnstead Easypure LFsystem.

Polymerization Apparatus. Figure 1a provides a schematic of the experimental reactor used in this research. Carbon dioxide and monomer were pumped using syringe pumps (Isco 260D). All feed lines have check-valves (HIP) to prevent backflow and rupture disks (HIP) for safety in case of overpressurization. The reactor is a 100-mL stainless steel stirred autoclave (Parr Instruments) with a turbine impeller to provide mixing of ingredients. The reactor is heated by a furnace, has an installed pressure transducer (Ashcroft K25F) and a thermowell containing a thermocouple (Parr-A472E2). Reactor temperature was controlled by a digital controller (Parr 4842). Control of the reactor temperature (T) and pressure (P) variation was excellent during a given experiment run ($T = \pm 0.5$ °C and $P = \pm 1$ bar).

Online Characterization. In situ FTIR monitoring of solution concentration in the stirred autoclave was performed using a high-pressure diamond immersion probe (Sentinel-ASI Applied Systems). The probe is attached to an ATR-FTIR spectrophotometer (ASI Applied Systems ReactIR 4000), connected to a microcomputer, supported by ReactIR software (ASI).

View Cell. An alternative for the autoclave is a 25-mL stainless steel view cell with sapphire windows (Figure 1b). This apparatus was similar in design to that reported on elsewhere.[11]

Polymerization Procedure. To determine the activity of the various acids (acetic, formic, benzoic, and chloroacetic) for catalyzing the condensation reaction, 20-mL acetone was added to all acids to aid in dissolution (benzoic and chloroacetic acid were not soluble in $scCO_2$ without this cosolvent). The acid, cosolvent, and orthosilicate monomer were added to the autoclave before heating and addition of carbon dioxide. In the second group of experiments, the acid (acetic or formic) was added to the autoclave before heating and addition of carbon dioxide to the desired pressure. Then TEOS (or TMOS) was

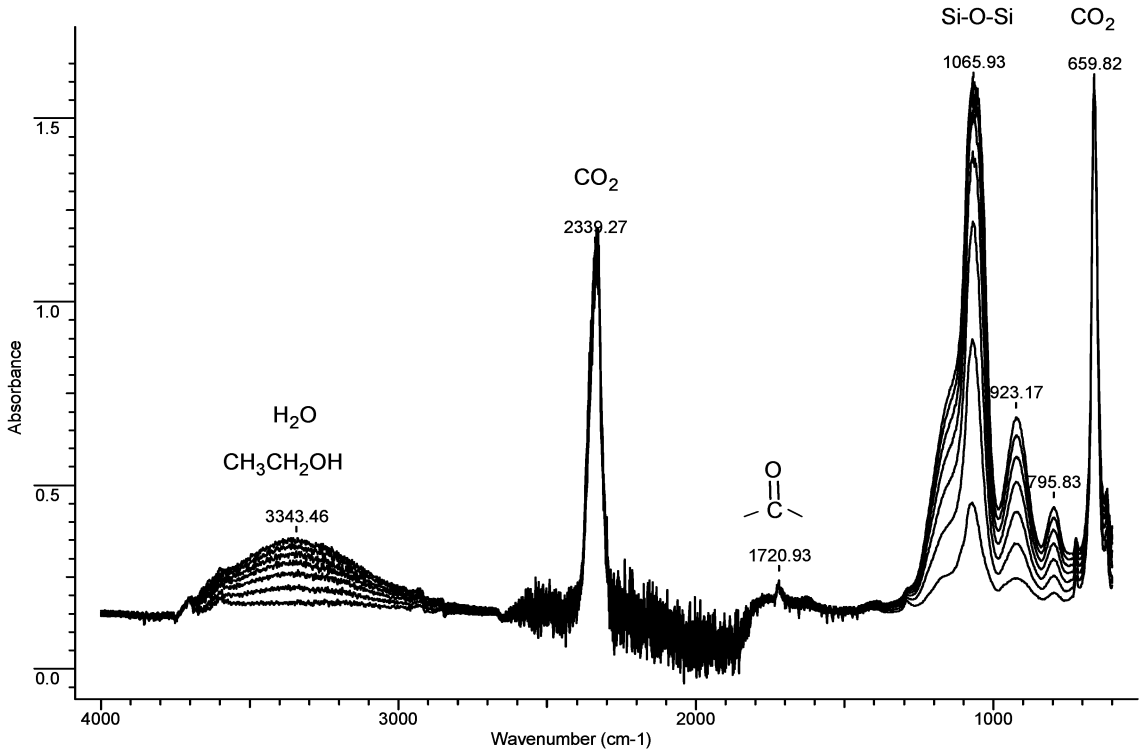

Figure 2. ATR-FTIR plot of the progress of an aerogel reaction in supercritical carbon dioxide, where the lines are experimental data: 4.4 mmol TEOS + 22 mmol HAc + 4.4 mmol H_2O at 3000 psig and 60 °C from 1 to 7 h at 1-h intervals.

pumped in with a separate syringe pump. FTIR spectra were obtained in situ, and GC-MS spectra were obtained by venting sample gas through a tube that connected the autoclave and the GC-MS. After reactions were completed, excess carboxylic acid was washed with fresh $scCO_2$ at a fixed venting rate (≈20 mL/min). The results provided were the mean of three separate experiments, and the error bars represent one standard deviation.

Particle Formation and Collection Techniques. Two techniques for particle formation were employed. One was direct formation of particles in the stirred reactor during depressurization with a fixed CO_2 venting rate. For the other one, the RESS process was used (see Figure 1c), where particles were sprayed through a variable-volume nozzle (HIP) into a closed stainless steel chamber with heating jacket (Parr Instruments) to collect particles sprayed at a constant depressurizing rate. The inlet of the particle collection device was connected to the stirred reactor and the outlet went through a filter (HIP) and was vented to a high velocity fume hood.

Characterization Techniques. Scanning electron microscopy (SEM) measurements were used to determine the size and morphology of particles. These measurements were made at either Surface Science Western on a Hitachi S-4500 FE instrument using an accelerating voltage of 5kV, or at the UWO Photonics and Nanotechnology Laboratory using a LEO 1530 Field Emission Scanning Electron Microscope. Solid aerogel powders were characterized by a Bruker Vector 22 FTIR instrument using a MIRacle Single Reflection HATR (Pike Technologies).

Results and Discussion

FTIR Analysis of Polymerization Reaction. Figure 2 provides a series of traces for a typical experiment in $scCO_2$, taken at fixed time intervals, from the in situ ATR-FTIR analysis of the condensation of TEOS using acetic acid. Analysis of the spectra shows that the absorptions at 1065, 928, and 797 cm^{-1} correspond to the stretching frequency of the Si−O−Si bond from the product,[32,33] whose concentration increases as the reaction proceeds. The produced silica aerogel powder was further analyzed by a separate offline FTIR instrument, which is designed for measuring solid materials. Figure 3 shows the results of this analysis, which confirm the peaks at 1065, 928, and 797 cm^{-1} belong to the aerogel product. The in situ FTIR analysis showed that the product peaks were found to increase during the course of the polymerization and then would remain constant if the reaction approached equilibrium, or the saturated concentration of polymer was reached. As mentioned in the Introduction, ATR-FTIR analysis is mainly sensitive to material dissolved in solution. This reaction was repeated in an agitated view-cell reactor, and the solution remained clear during the course of the condensation reaction. As the condensation product is most likely polydisperse with a broad range of molecular weights, it is not possible to directly determine concentration of the molecules by FTIR, only of the actual bond concentration. Analysis of the FTIR spectrum also shows a product peak at 3344 cm^{-1}, which increases during the course of the reaction from the production of the condensate molecule. The condensate molecule is a mixture of H_2O and CH_3CH_2OH. Both the alcohol and water will merge into an indistinguishable broad peak in this range.

Activity of Various Acids. To compare the relative activity of the various acids studied in the condensation of orthosilicates, the main absorbance from the product at 1066 cm^{-1} was plotted versus reaction time (see Figure 4). The results showed that among the four acids, benzoic and chloroacetic acid were the most active in promoting conversion to product. However, several problems make these acids poor candidates for the polymerization agent. First, as we will see later, slower condensation of orthosilicates is preferred to form discrete particles. Second, as both of these acids are solid at room temperature, and as they have poor solubility in $scCO_2$, this

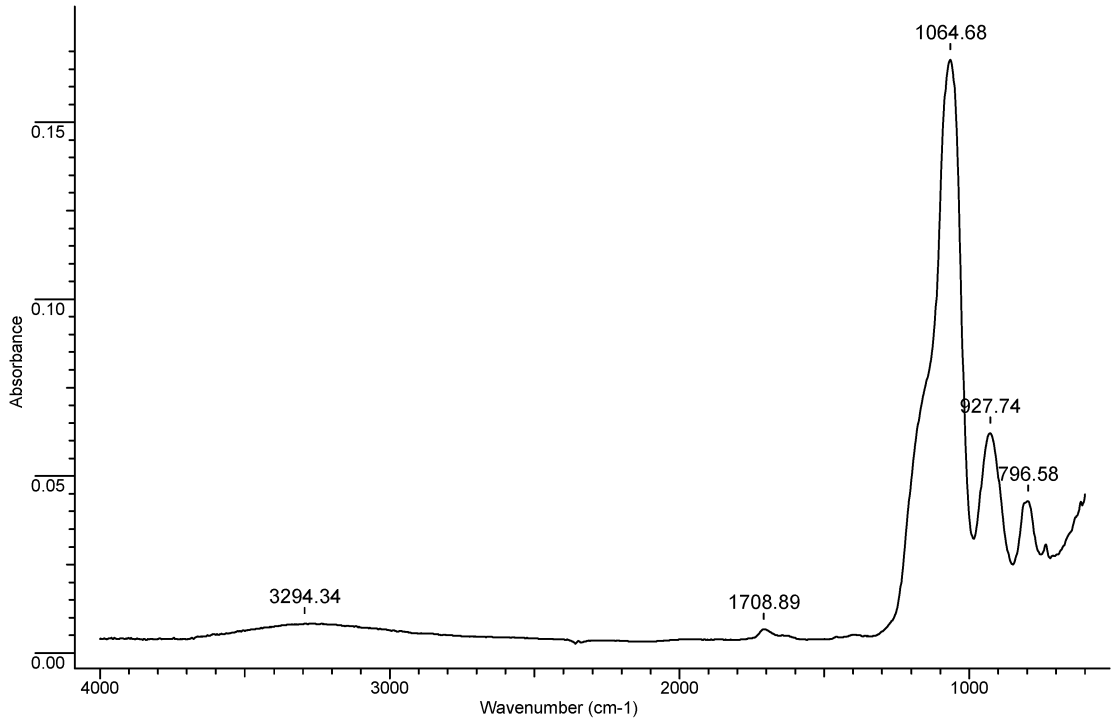

Figure 3. FTIR plot of the silica aerogel powder, where the line is experimental data. The spectrum was taken at ambient conditions.

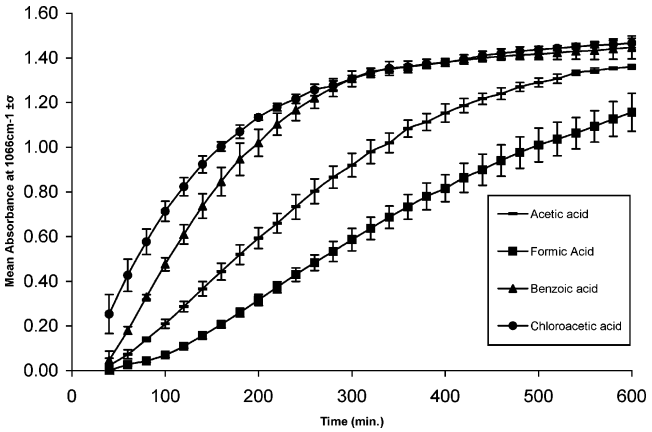

Figure 4. Effect of acid type on TEOS condensation activity in supercritical CO_2. The points are experimental data from the ATR-FTIR absorbance at 1066 cm^{-1} ($n = 3$) and the lines are best-fit smoothed lines through the data points: acetic acid (—), formic acid (■), benzoic acid (▲), and chloroacetic acid (●). The experimental conditions are 60 °C and 3000 psig, 0.0044 mol TEOS, 0.0176 mol acid, and 0.275 mol acetone.

makes separation from the final product difficult. Both anhydrous acetic and formic acids were less active than the other two acids. At 10 h of reaction at 60 °C and 3000 psig, the absorbance at 1066 cm^{-1} was still increasing, indicating that the equilibrium of the polymerization had not yet been reached.

Figure 5 shows that production of the condensation product could rise remarkably by addition of (a) a small amount of water (Alkoxysilane: $H_2O = 1 \sim 2$) or (b) more acid. NMR studies in aqueous sol−gel polymerizations show similar accelerations with increased concentrations of water.[34] However, too much water was found to make the reaction rate too high, causing precipitation and agglomeration of aerogel particles. Also, too much acid is not economically feasible and causes downstream separation problems.

Effect of Temperature and Pressure. Figure 6 shows that higher temperatures resulted in significantly higher polymerization rates. The rate of condensation clearly increases with temperature, as one would expect.[35] Figure 7 shows an interesting effect from experiments varying the reactor pressure. Increasing the reactor CO_2 pressure caused lower initial reaction rates, but led to higher final concentrations. Similar results were found when the agitation rate was tripled from 200 to 640 rpm, indicating the reactions are not likely mass-transfer limited for these conditions. At lower pressures, such as the case for the experiment performed at 1300 psig, the low density of CO_2 near the critical point causes increased relative concentrations of orthosilicate and acid in certain "clusters". This clustering can increase the rate of reaction.[36] The higher absorbance values observed at higher pressures may be explained by increased solubility of the reaction products.

Experimental Phase Behavior. Using the view-cell system for the experimental conditions studied, it was found that TMOS, TEOS, acetone, acetic acid, and formic acid were miscible with CO_2. Benzoic and chloroacetic acid had poor solubility, but were soluble in CO_2 with added acetone cosolvent. When the FTIR experimental conditions were further examined by means of the view cell reactor, it was found that precipitates appeared spontaneously after the silicon alkoxide and 96% formic acid (≈4% water) were pressurized with $scCO_2$ and heated. Figure 8 shows an example of the typical agglomerated micron size spheres that were produced. The situation could be improved by adding excess formic acid as cosolvent in $scCO_2$, and by decreasing the concentration of reactants (Figure 9), but precipitation of the products was still inevitable. However, when using anhydrous acetic or formic acid and small amounts of water (water/alkoxysilane = less than 2/1), the fluid remained clear, indicating that the products remained in solution.

Particle Formation. Particles were formed either by depressurizing the reactor vessel or expanding the particles, using a modified RESS process, into a heated collection chamber. When depressurizing the reactor vessel, particles would form at pressures of approximately 900 ∼ 1000 psig. Results from the view cell observation and SEM showed that separated micro-

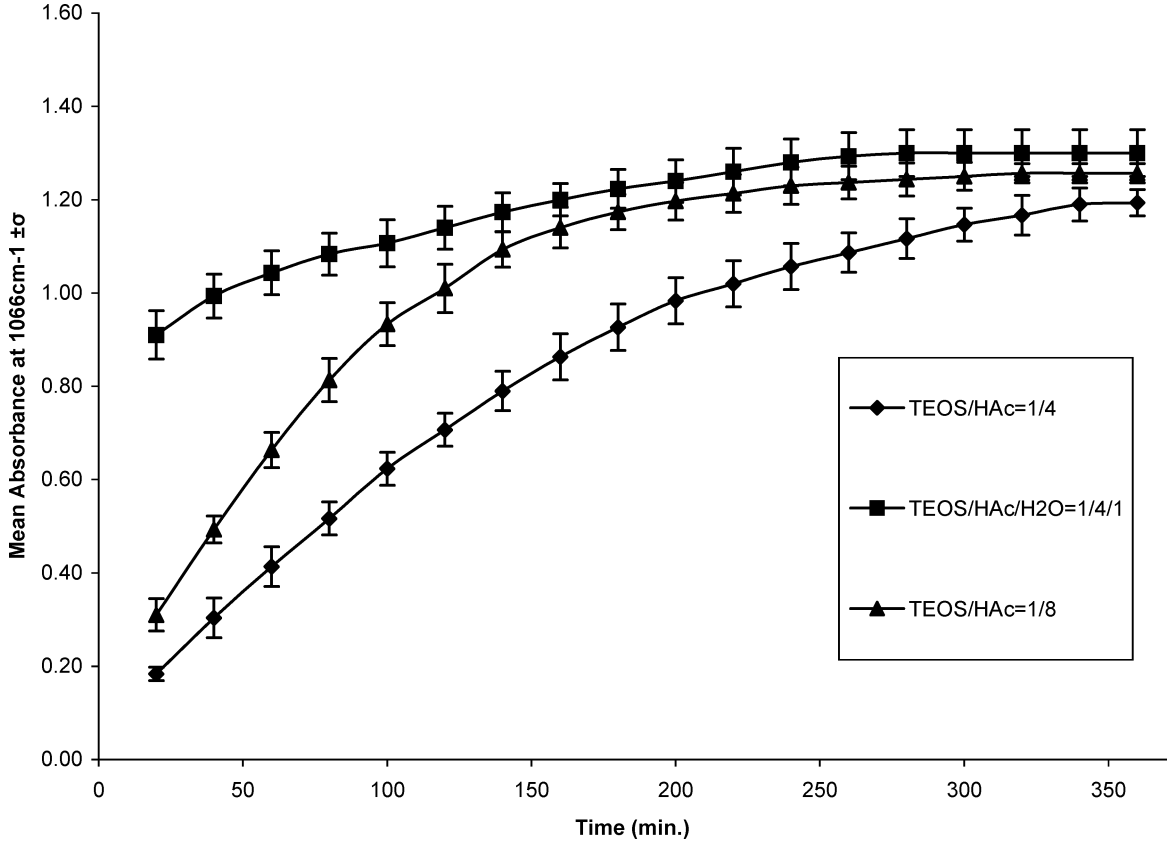

Figure 5. Effect of water and acid concentration on TEOS condensation activity in supercritical CO_2. The points are experimental data from the ATR-FTIR absorbance at 1066 cm^{-1} ($n = 3$) and the lines are best-fit smoothed lines through the data points. 0.0088 mol TEOS + 0.0352 mol HAc (●); 0.0088 mol TEOS + 0.0352 mol HAc + 0.0088 mol H_2O (■); 0.0088 mol TEOS + 0.0704 mol HAc (▲). The experimental conditions are 50 °C and 3000 psig.

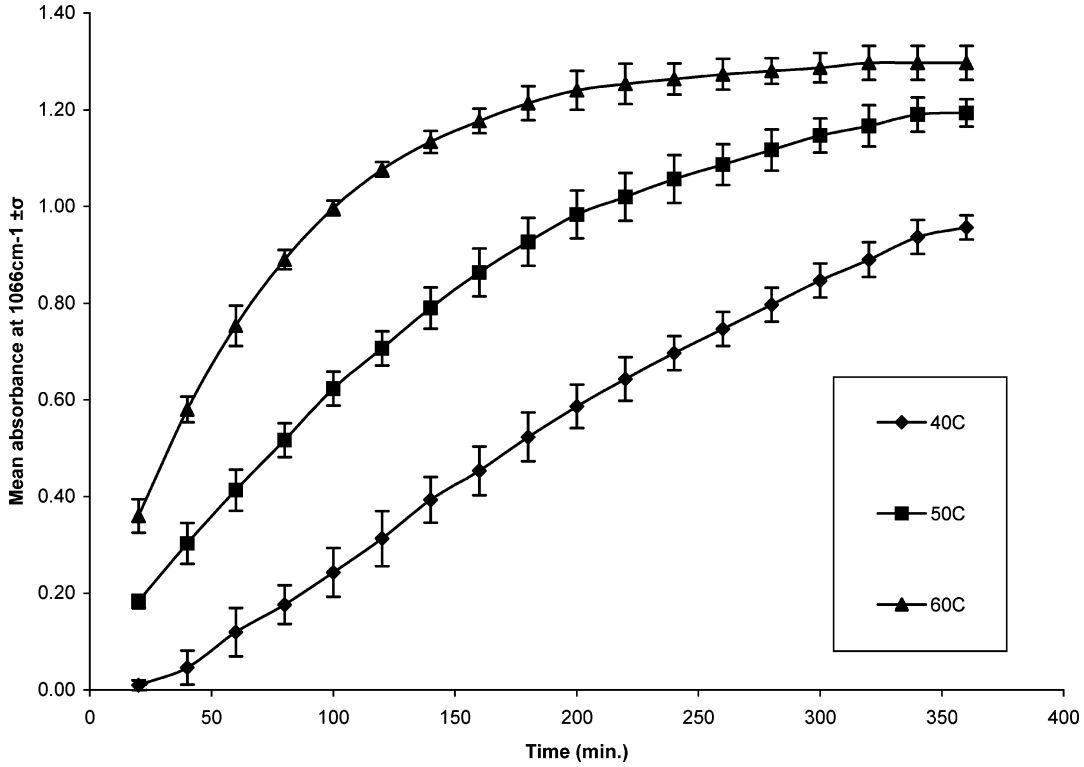

Figure 6. Effect of temperature on TEOS condensation activity in supercritical CO_2. The points are experimental data from the ATR-FTIR absorbance at 1066 cm^{-1} ($n = 3$) and the lines are best-fit smoothed lines through the data points: 40 °C (●); 50 °C (■); 60 °C (▲). The experimental conditions are 3000 psig, 0.0088 mol TEOS, and 0.0352 mol acetic acid.

spheres were formed when the pressure dropped to about 900 ~ 1000 psig. When using the modified RESS process, the particle size was found to decrease with increasing rate of depressurization and the particles were significantly smaller than

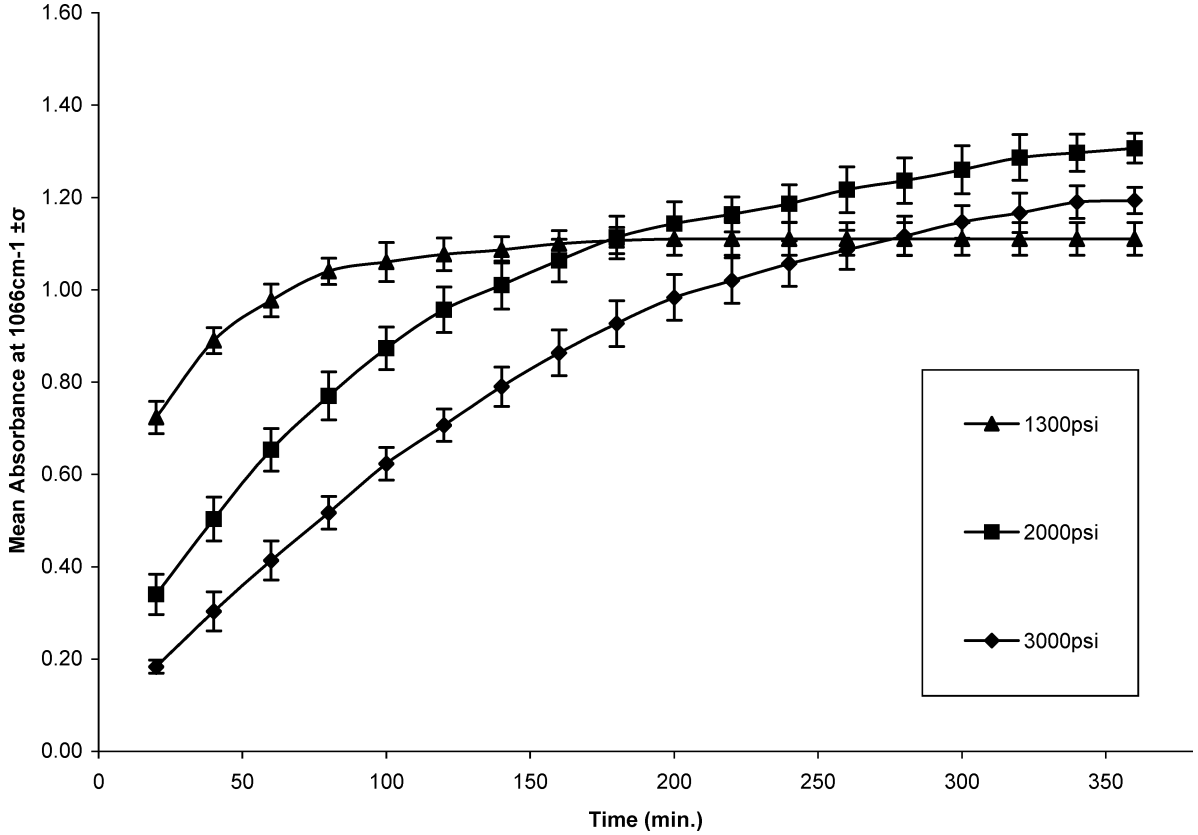

Figure 7. Effect of pressure on TEOS condensation activity in supercritical CO_2. The points are experimental data from the ATR-FTIR absorbance at 1066 cm^{-1} ($n = 3$) and the lines are best-fit smoothed lines through the data points: 3000 psig (●); 2000 psig (■); 1300 psig (▲). The experimental conditions are 50 °C, 0.0088 mol TEOS, and 0.0352 mol acetic acid.

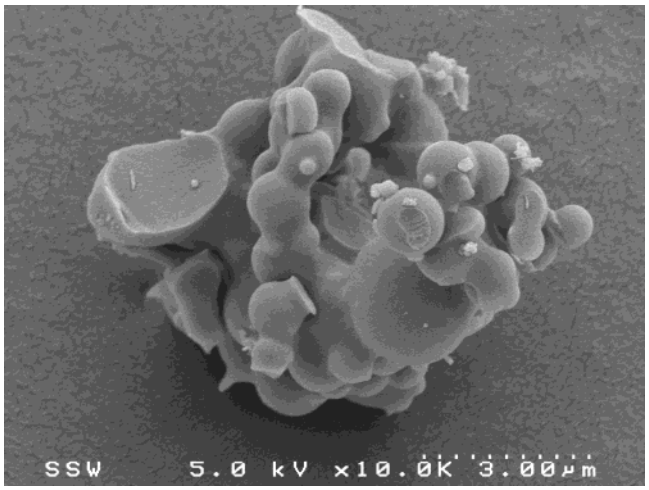

Figure 8. SEM of silica aerogel powder. The experimental conditions are 1.1 mmol TEOS + 7.7 mmol 96% HCOOH in the 25-mL view cell, at 2000 psig, 40 °C.

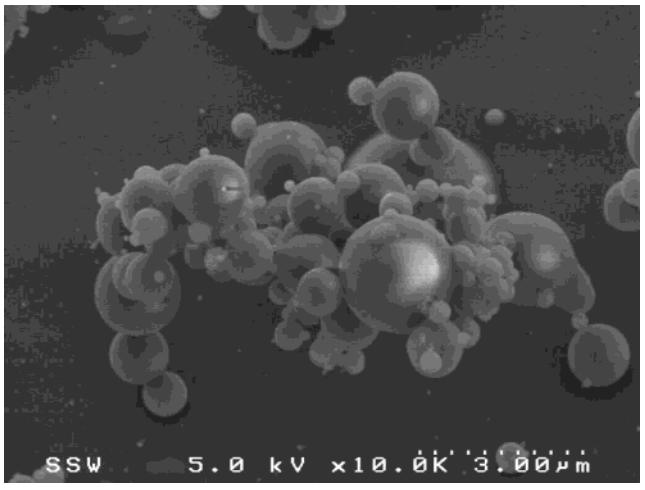

Figure 9. SEM of silica aerogel powder. The experimental conditions are 0.176 mmol TEOS + 2.64 mmol 96% HCOOH in the 25-mL view cell, at 2000 psig, 40 °C.

those formed from depressurizing the reactor vessel. Generally, a higher venting rate made smaller particles with narrower distributions and lower levels of agglomeration. The particles gathered in the autoclave, spheres in the range between submicron and several microns (Figure 10), were larger than those formed in the device outside the autoclave by the RESS process (with approximate diameters of 100 nm) (Figure 11).

Future work will be directed at a better understanding of the kinetics of the sol−gel polymerization mechanism in $scCO_2$, and the mechanism of particle formation. A knowledge of these can provide for a one-step mechanism to produce nanoceramic particles from SCFs.

Conclusions

This study of the particle formation process for aerogels in supercritical carbon dioxide demonstrated that in situ ATR-FTIR spectroscopy is a valuable technique for studying this high-pressure process. Both anhydrous formic and acetic acid were found to be mild and controllable agents for sol−gel route preparation of silica aerogel particles in $scCO_2$. By modifying the ratio of silicon alkoxide, acetic acid, and water, the polymerization rate is tunable and precipitation can be prevented, and therefore agglomeration minimized. Increasing the reaction temperature led to higher rates of reaction and increasing the pressure decreased the rate of reaction. Submicron particle sizes

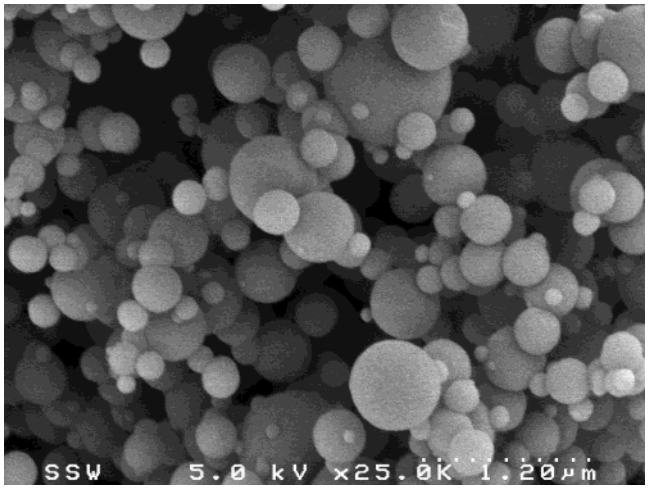

Figure 10. SEM of silica aerogel powder collected from the high-pressure mixer upon decompression. The experimental conditions are 0.0044 mol TEOS + 0.0176 mol HAc, 3000 psig, 60 °C.

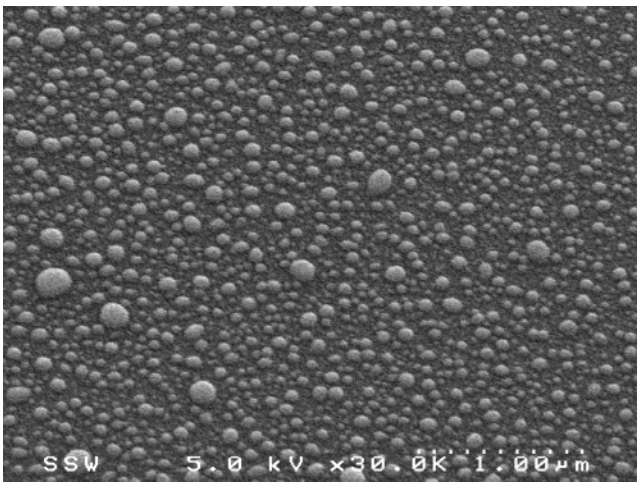

Figure 11. SEM of silica aerogel powder collected using the Rapid Expansion of Supercritical Solutions (RESS) process. The experimental conditions are TEOS/HAc = 1:4 6000 psig, 60 °C.

were obtained when the sol−gel solution was destabilized by pressure reduction. Particles as small as 100 nm were formed using the RESS process.

Acknowledgment. We would like to thank Dr. Xingsheng Li for his help on GC-MS. We thank Mr. Brad Kobe and Surface Science Western, along with Dr. Ian Mitchell and the UWO Photonics and Nanotechnology Laboratory, for use of the Scanning Electron Microscope. This work was financially supported by the Canadian Natural Science and Engineering Research Council (NSERC) and by the Materials and Manufacturing Ontario EMK program.

References and Notes

(1) Cooper, A. I. *Adv. Mater.* **2001**, *13*, 1111.

(2) Cansell, F.; Chevalier, B.; Demourgues, A.; Etourneau, J.; Even, C.; Garrabos, Y.; Pessey, V.; Petit, S.; Tressaud, A.; Weill, F. *J. Mater. Chem.* **1999**, *9*, 67.

(3) Woods, H. M.; Silva, M. C.; Nouvel, C.; Shakesheff, K. M.; Howdle, S. M. *J. Mater. Chem.* **2004**, *14*, 1663.

(4) Kendall, J. L.; Canelas, D. A.; Young, J. L.; DeSimone, J. M. *Chem. Rev.* **1999**, *99*, 543.

(5) Charpentier, P. A.; DeSimone, J. M.; Roberts, G. W. Continuous Polymerizations in Supercritical Carbon Dioxide. In *Clean Solvents*; Abraham, M. A., Moens, L., Eds.; ACS Symposium Series: Washington, DC, 2002; Chapter 9, p 113.

(6) Hitzler, M. G.; Poliakoff, M. *Chem. Commun.* **1997**, 1667.

(7) Ye, X.; Wai, C. M. *J. Chem. Educ.* **2003**, *80*, 198.

(8) Denison, G. M. J.; Charles, A.; DeYoung, J.; Gross, S. M.; McClain, J.; Zannoni, L. A.; Hicks, E.; Wood, C. D.; Boggiano, M. K.; Visintin, P. M.; Bessel, C. A.; Schauer, C. K.; DeSimone, J. M. *PMSE* **2004**, *90*, 152.

(9) Royer, J. R.; Siripurapu, S.; DeSimone, J. M.; Spontak, R. J.; Khan, S. A. *PMSE* **2001**, *84*, 276.

(10) DeSimone, J. M.; Tumas, W. *Green Chemistry Using Liquid and Supercritical Carbon Dioxide*; Oxford University Press: New York, 2003.

(11) McHugh, M. A.; Krukonis, V. J. *Supercritical Fluid Extraction: Principles and Practice*, Second ed.; Butterworth-Heinemann: Boston, 1994.

(12) Debenedetti, P. G.; Tom, J. W.; Kwauk, X.; Yeo, S.-D. *Fluid Phase Equilib.* **1993**, *82*, 311.

(13) Tan, H. S.; Borsadia, S. *Exp. Opin. Ther. Patents* **2001**, *11*, 861.

(14) Gallgher, P. M., Krukonis, V. J., Botsaris, G. D. I., Eds.; Gas anti-solvent recrystallization: Application to particle design. In *Particle Design via Crystallization*,; Ramanarayanan, R., Kern, W., Larson, M., Sidkar, S., Eds.; AICHE symp. Ser. 284, 1991; p 96−103.

(15) Jung, J.; Perrut, M. *J. Supercrit. Fluids* **2001**, *20*, 179.

(16) Turk, M. *J. of Supercritical Fluids* **1999**, *15*, 78.

(17) Stanton, L. A.; Dehghani, F.; Foster, N. R. *Aust. J. Chem.* **2002**, *55*, 443.

(18) Helfgen, B.; Hils, P.; Holzknecht, C.; Turk, M.; Schaber, K. *Aerosol Sci.* **2001**, *32*, 295.

(19) Subra, P.; Jestin, P. *Powder Technol.* **1999**, *103*, 2.

(20) Ye, S. *Can. J. Chem.* **1997**, *75*, 1666.

(21) Hair, L. M.; et al. *J. Non-Cryst. Solids* **1995**, *186*, 168.

(22) Hrubesh, L. W. *J. Non-Cryst. Solids* **1998**, *225*, 335.

(23) Schmidt, M.; Schwertfeger, F. *J. Non-Cryst. Solids* **1998**, *225*, 364.

(24) Kistler, S. S. *Nature* **1931**, *127*, 741.

(25) Kistler, S. S. *J. Phys. Chem.* **1932**, *36*, 52.

(26) Brinker, C. J.; Scherer, G. W. *Sol−Gel Science*; Academic Press: New York, 1990.

(27) Cooper, A. I. *J. Mater. Chem.* **2000**, *10*, 207.

(28) Loy, D. A.; Russick, E. M.; Yamanaka, S. A.; Baugher, B. M. *Chem. Mater.* **1997**, 7499.

(29) Moner-Girona, M.; Roig, A.; Molins, E.; Llibre, J. *J. Sol-Gel Sci.* **2003**, *26*, 645.

(30) Feng, L.; Berglund, K. A. *J. Cryst. Growth* **2002**, *2*, 449.

(31) Lewiner, F.; F'evotte, G.; Klein, J. P.; Puel, F. *J. Cryst. Growth* **2001**, *226*, 348.

(32) Tohge, N.; Moore, G. S.; Mackenzie, J. D. *J. Non-Cryst. Solids* **1984**, *63*, 95.

(33) Dean, J. A. *Analytical Chemistry Handbook*; Academic Press: New York, 1995.

(34) Pouxviel, J. C.; Boilot, J. P.; Beloeil, J. C.; Lalleman, J. Y. *J. Non-Cryst. Solids* **1987**, *89*, 345.

(35) Odian, G. *Principles of Polymerization*, 3rd ed.; John Wiley & Sons: New York, 1991.

(36) Kim, S.; Johnston, K. P. *AIChE J.* **1987**, *33*, 1603.